UCRL-15046

SOME FEATURES OF RAYLEIGH SCATTERING FROM LIGHT ATOMS AND IONS

J. C. Parker, R. H. Pratt

July 18, 1979

P.O. 9776405

DEPARTMENT OF PHYSICS AND ASTRONOMY
UNIVERSITY OF PITTSBURGH
PITTSBURGH, PENNSYLVANIA

PITT-215
INTERNAL REPORT
June 1979

Some Features of Rayleigh Scattering from Light Atoms and Ions*

John C. Parker and R. H. Pratt

Department of Physics and Astronomy
University of Pittsburgh
Pittsburgh, Pennsylvania 15260

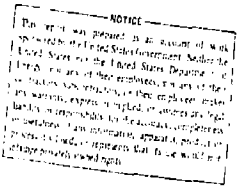

Abstract

When photon energies are well below 1 MeV the only significant contribution to elastic (coherent) photon-atom scattering comes from Rayleigh scattering, the elastic scattering of photons from bound atomic electrons. This report discusses the Rayleigh scattering cross sections for atoms and ions of low nuclear charge, particularly for photon energies in the vicinity of the threshold for photoionization from the K-shell. Just below this threshold energy there is a sequence of resonances in the elastic scattering amplitude. Each resonance occurs at an energy corresponding to the excitation of a K-shell electron to a higher unfilled shell. For a multi-electron atom the total cross section can go through a near zero minimum just below the resonance region due to interference between K and L amplitudes. The resonance region expands with increasing ionization, on the low side as more interior shells become unfilled and accessible, and, on the high side as the ionization threshold increases. Above the ionization threshold, in an isonuclear sequence the K-shell amplitudes share a common curve differing only in the position of the threshold. When the K-shell is opened the amplitude departs from this common curve. Above, but near, threshold the imaginary part of the K-shell amplitude is important but it rapidly decreases. Well above the threshold form factor predictions are approached for the atom and for the scattering from each subshell separately.

* Prepared for the Lawrence Livermore Laboratory of the University of California under contract number 9776403.

We here report the results of a study of Rayleigh scattering from light atoms and ions and indicate directions in which further work is needed. We confine our attention in this discussion to photon energies in the vicinity of the K-shell's photoionization threshold.

Rayleigh scattering is the elastic scattering of photons from bound atomic electrons. For photon energies below 1 MeV the only significant contribution to elastic photon-atom scattering comes from Rayleigh scattering. For photon energies above 100 eV and below about 1 keV the Rayleigh amplitudes have essentially a dipole character, and hence a simple angular shape. The amplitudes become less like dipole as the energy is increased, as can be seen in Figs. 1a, 2, and 3a, where the backward scattering cross section falls away from the forward scattering cross section with increasing energy. (If the amplitudes were purely dipole the backwards and forward cross sections would be equal.) In the situation where the amplitudes are essentially dipole, for a given photon energy there is only one independent quantity (with real and imaginary parts) which may be taken as the no spin-flip amplitude for forward scattering. If one chooses to express photon polarization in terms of components parallel ($A_{//}$) and perpendicular ($A_{\perp}$) to the plane of scattering, dipole approximation corresponds to the statement that for fixed energy

$A_{\perp}$ = constant, and

$A_{//} = A_{\perp} \cos\theta$, where θ is the scattering angle.

The details of our numerical procedures for calculating Rayleigh scattering amplitudes in a central field approximation have been given previously.[1] A relativistic HFS potential has been used in a formalism which assumes that atomic processes proceed through single electron transition in a central potential common to all electrons.

The total atom amplitude for Rayleigh scattering is the sum of the scattering amplitudes for scattering off the electrons of each subshell. In an approximation in which all electrons share a common potential the individual subshell amplitudes can be computed independently, without regard for the occupation of other subshells to which virtual transitions may be made during the process. Treating the subshells independently, in this manner, introduces into the subshell amplitude resonances corresponding to every transition from a given subshell to any other. The resonances corresponding to transition to unfilled shells are real and will appear in the physical total atom amplitude. This region of resonances will in general differ from ion to ion thus forming a "signature" of the ion analogous to its spectrum. The region will expand with increasing ionization, on its lower edge as more interior shells become unfilled and accessible, and on its upper edge as the ionization threshold increases. The region will also expand with increasing nuclear charge as the intervals between bound state energies increase. Furthermore, the region will move as a whole to higher energy as the threshold energy increases as it will with increasing ionization or nuclear charge.

Resonances corresponding to a transition to a filled shell are fictitious and cancel in the sum over subshell amplitudes. For example, in Fig. 4, the K L_{II} and L_{III} amplitudes of neutral Neon have resonances at the K-$L_{II,III}$ transition energy of 0.814 keV, but the physical total atom amplitude has no such resonance, being smooth through the K-$L_{II,III}$ transition energy. (The total atom amplitude has its first resonance slightly above 0.820 keV, corresponding to the K-M transition energy.) Carbon has a real resonance at its K-$L_{II,III}$ transition energy (see Fig. 1).

To illustrate the behavior of the Rayleigh amplitude near the K-edge we will use Carbon and Neon as examples. From our numerical data for neutral

Carbon and from Gavrila's nonrelativistic dipole calculation for Hydrogen[2] we have good descriptions of the Rayleigh amplitudes for neutral Carbon and H-like Carbon (C^{+5}). We have verified in some cases that for low photon energy (W) Gavrila's results as a function of W/E_K where E_K is the K-shell binding energy, agree to a few percent with relativistic Coulomb calculations performed with our code. We can infer the general features of the K-shell and total atom Carbon isonuclear sequence cross sections from these two limiting cases and then verify them through direct calculation. But while we will present some ionic data of this type we have concluded (as is explained below) that the present Rayleigh code needs modification for ions at low energy before it is run extensively.

Gavrila's calculation is an analytic calculation in the nonrelativistic dipole approximation using hydrogenic wave functions. This calculation derives an exact analytic formula for the Kramers-Heisenberg matrix element in terms of the Green's function for the Coulomb field. Thus, unlike most earlier work, the calculation includes the $p \cdot A$ as well as the A^2 term of the nonrelativistic matrix element and hence exhibits the correct behavior of the amplitudes in the resonance region. Gavrila's results are shown in Fig. 5. The abscissa is $k = W/E_K$, where W is the photon energy and E_K is the K-binding energy. The ordinate is the scattering amplitude (per electron) in units of the classical electron radius r_e. The amplitude vanishes when $k \to 0$ as k^2, and grows as k increases towards the first resonance at $k = 0.75$. Between 0.75 and threshold the amplitude has an infinite number of resonances at energies of the dipole-allowed bound-bound transitions from the K-shell. Above threshold the Rayleigh amplitude has both real and imaginary parts, comparable in magnitude near threshold for these low Z cases. The imaginary part is directly related to the photoeffect cross section (σ_{photo}):

$$\sigma_{photo}(W) = \frac{4\pi}{W} \text{ Im } A_{\parallel}(W, \theta=0) = \frac{4\pi}{W} \text{ Im } A_{\perp}(W, \theta=0). \qquad (1)$$

Like the photoeffect cross section, the imaginary part decreases monotonically from its threshold value. The real part, which is always close to 1.0 r_e in value above threshold rises to a gentle maximum of 1.23 for k = 1.548 and then gradually falls to the form factor value of 1.0.

The qualitative features seen in the Hydrogenic calculation appear also in the amplitudes for subshells of other atoms. In our numerical data (Fig. 1) for neutral Carbon we can see the first resonance below the K-edge. The limitations of our present numerical methods do not allow us to resolve the higher resonances. (In its current form the Rayleigh code, in terms of its design for calculating low energy continuum states, fails for energies within a few eV of a resonance.)

The resonances are infinite because in this approximation the finite widths of unoccupied levels are ignored.

Above threshold the K-shell Rayleigh amplitude for neutral Carbon and Neon (Fig. 6) has an interesting turnover just above threshold. In the real part this turnover is obvious in the Neon data and appears to be just on threshold for neutral Carbon; in the imaginary part it is just beginning for Neon.

For higher energies the K-shell Rayleigh amplitudes show the same trends as in the hydrogenic case: the imaginary part steadily declines, and the real part approaches form factor predictions after a gentle maximum. (Note that there are now <u>two</u> K-shell electrons.)

When the K-shell amplitudes for the isonuclear sequence are plotted for photon energies above threshold (Fig. 7) the amplitudes with filled K-shells share a common curve. (The slight divergence of the C^{+4} data from this

curve near the C^{+4} threshold may be due to problems with the numerical code and not a real physical effect. See also the kink in the C^{+4} cross sections in Fig. 2 which also suggests a problem with the code.) Only the positions of the threshold vary, moving to higher energy with increasing ionization. When the K-shell is opened, the K-shell amplitude, apart from the decrease due to the lower occupation, rises slightly above the general curve. The amplitudes in Fig. 7 are plotted with the same occupation 2 in each case. (The amplitude for hydrogenic Carbon is half that shown.) Given the intimate connection via the optical theorem between Rayleigh scattering and photoeffect it is not surprising that precisely the same behavior is observed in ionic photoeffect from an isonuclear sequence.[3] In both cases the explanation is that the matrix element is being determined in the interior of the atom, where the only effect on the shape of the potential due to removal of outer electrons is a constant energy shift. The L-shell amplitudes (and higher shell amplitudes for atoms with more than ten electrons) should be smooth through the K-edge, if the K-shell is full. However, since we calculate subshell amplitudes independently, we introduce into the L-amplitudes a "fictitious" resonance as discussed above. Except for this resonant component, the L-shell amplitude is within a few percent of the form factor for energies corresponding to ionization of the K-shell and above.

Near the L-K resonance

$$A_L \simeq A_L^{FF} + \frac{\langle L|\hat{\varepsilon}_f \cdot \vec{\alpha} e^{i\vec{k}_f \cdot \vec{r}}|K\rangle \langle K|\hat{\varepsilon}_i \cdot \vec{\alpha} e^{i\vec{k}_i \cdot \vec{r}}|L\rangle}{W - E_{KL}} \qquad (2)$$

where W is the photon energy, E_{KL} is the K → L transition energy, $\vec{k}_f$ and $\vec{k}_i$ are the final and initial photon momenta, $\hat{\varepsilon}_f$ and $\hat{\varepsilon}_i$ are the final and initial photon polarizations, and A_L^{FF} is the form factor amplitude.

For $L_I(2s_{1/2})$ the second term in (2) is small except right on resonance since K-L_I is dipole forbidden. For $L_{II}(2p_{1/2})$ and $L_{III}(2p_{3/2})$ this term dominates when $|W-E_{KL}| \lesssim 10$ eV. The resonant term could be extracted by fitting to a $\frac{1}{W-E_{KL}}$ form very near resonance, and then subtracting. There is, however, always some ambiguity in such a numerical fit. In order to obtain more precise results, more suitable for smooth interpolation procedures, efforts are now under way to calculate the two terms of the matrix elements in (1), so that the resonant and non-resonant terms can be treated unambiguously.

As we have noted in the beginning, the total atom amplitude contains the observable physics, illustrated for the C, C^{+4} and Ne cross sections at 0°, 90° and 180° in Figs. 1, 2 and 3. For H and He the K-shell amplitude multiplied by the fractional occupation is the total atom amplitude. When an L-shell is occupied, however, the K and L amplitudes interfere constructively above the K-edge and destructively below. Below the K-edge the K-shell amplitudes are opposite in sign from the L-amplitudes (and the higher shell amplitudes as well). Well below the K-edge the outer shells dominate, as the K-amplitude is very small. As W approaches the first <u>real</u> resonance from below the actual K-amplitude (ignoring fictitious resonances) grows as $\frac{1}{W-E_{Res}}$, and hence will at some energy cancel the real part of the sum of the outer shell amplitudes which are slowly varying. This cancellation sends the cross section through a near zero minimum, finite because the K-amplitude has no imaginary part (except at the resonance transitions) which could cancel the imaginary part of the outer shell amplitudes. Beyond this minimum the K-amplitude is growing rapidly (as $\frac{1}{W-E_{Res}}$) and soon dominates the contribution of the outer shells.

Fig. 1 shows the minimum for Carbon immediately below the resonance at the $K\text{-}L_{II,III}$ energy. In Fig. 3 the Neon cross section has yet to reach

the minimum. It will be noticed that the minimum in Neon occurs beyond the $K\text{-}L_{II,III}$ energy which demonstrates that the "fictitious" resonances as having no effect on this feature. They have been entirely cancelled. If data of sufficient resolution were available, the K-M resonances would appear in both the Carbon and Neon data. Furthermore, between each pair of resonances the real part of the total atom amplitude will again vanish because the K-shell amplitude changes sign on passing a resonance, and in this approximation goes from $-\infty$ to $+\infty$ between any two adjacent resonances while the outer shell amplitudes vary slowly. Therefore, between the first real resonance in the coherent scattering cross section and the photoionization threshold will be a sequence of resonances as in the hydrogenic case.

Above threshold the total atom cross sections for neutrals grow from a fairly small threshold value till it peaks at roughly twice the threshold energy. Then it falls to the form factor predictions from above. This is clearly a screening effect. Neither H-like Carbon nor He-like Carbon exhibit this maximum. It is probably related to the turnover in the K-shell amplitude mentioned above. However, further study is required before this maximum is understood.

While our present numerical code works efficiently for neutral species, for ionic cases it requires some modification. The basic formulation, both analytic and numerical, is still sound. The technical difficulty resides in the asymptotic fitting procedure used to normalize continuum wave functions, needed for an intermediate step in the calculation (related to the virtual intermediate states which are accessible in between photo-emission and absorption). The existing code matches the numerical wave function at large distances to a plane wave with a logarithmic phase factor, in the asymptotic region of the wave function. The continuum wave function is placed on high

speed storage (disk) for later use. However, for ions the electrons are in a very extended Coulomb well, which requires calculating continuum wave functions to very large distances before a Coulomb-plane wave is approached. (In one extreme case the wave function had to be computed out to several miles in real distances before such an asymptotic fit could be made.)

We are currently modifying the Rayleigh code so that continuum wave functions are matched to linear combinations of regular and irregular relativistic Coulomb wave functions (rather than their asymptotic plane wave forms) outside the ion.

This new version of the code has been written and is now being tested. We propose to use this version to continue the study of Rayleigh scattering from ions.

References

1. L. D. Kissel and R. H. Pratt, submitted to Phys. Rev. A.

2. M. Gavrila, Phys. Rev. 163, 147 (1967).

3. D. J. Botto, J. McEnnan and R. H. Pratt, Phys. Rev. A18, 580 (1978).

Figure Captions

Fig. 1. Total atom Rayleigh scattering differential cross sections for neutral Carbon in classical electron radii squared at (a) 0° and 180°, and (b) 90°. There is a resonance at the $K\text{-}L_{II,III}$ transition energy (0.264 keV).

Fig. 2. Total atom Rayleigh scattering differential cross sections for helium-like Carbon (C^{+4}) in classical electron radii squared at 0°, 90° and 180° above the photoionization threshold.

Fig. 3. Total atom Rayleigh scattering differential cross sections for neutral Neon in classical electron radii squared at (a) 0° and 180°, and (b) 90°.

Fig. 4. Forward Rayleigh scattering differential amplitudes for neutral Neon. The total atom amplitude (dashed curves) is continuous through the $K\text{-}L_{II,III}$ transition energy where the subshell amplitudes (solid curves) calculated by our method have resonances.

Fig. 5. Hydrogenic Rayleigh scattering forward differential amplitudes per electron as calculated in the non-relativistic dipole approximation by M. Gavrila (Ref. 2).

Fig. 6. K-shell forward differential Rayleigh scattering amplitudes for neutral Neon and Carbon vs. the ratio of photon energy (W) to K-binding energy (E_K) above the K-edge.

Fig. 7. K-shell Rayleigh forward differential amplitudes in classical electron radii for the isonuclear sequence of Carbon.

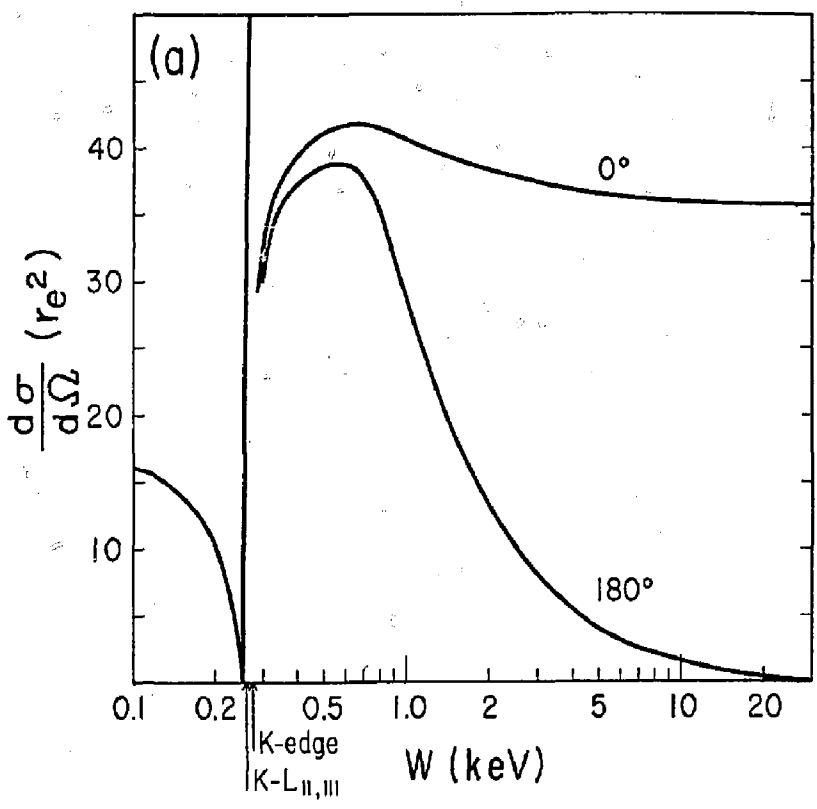
(a)
40
30
20
10
$\frac{d\sigma}{d\Omega}$ (r_e^2)
0°
180°
0.1
0.2
0.5
1.0
2
5
10
20
K-edge
K-L$_{II,III}$
W (keV)

Fig. 1(a)

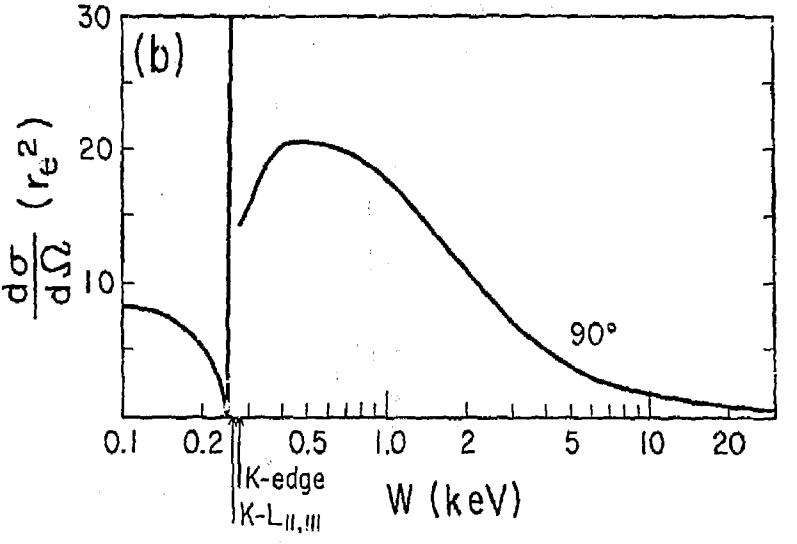
30
(b)
20
10
$\frac{d\sigma}{d\Omega}$ (r_e^2)
90°
0.1
0.2
0.5
1.0
2
5
10
20
K-edge
K-$L_{II,III}$
W (keV)

Fig. 1(b)

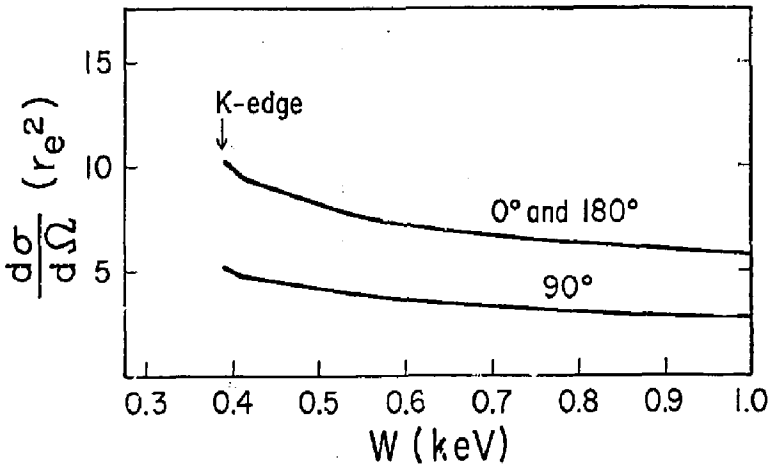

Fig.2

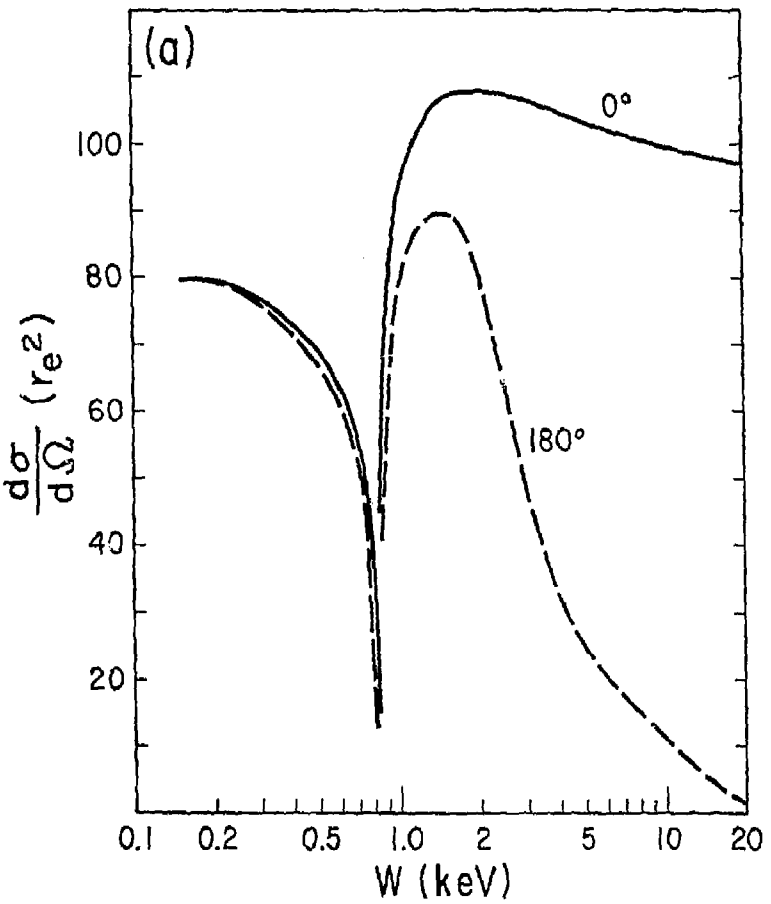
(a)
0°
180°
100
80
60
40
20
$\frac{d\sigma}{d\Omega}$ (r_e^2)
0.1
0.2
0.5
1.0
2
5
10
20
W (keV)

Fig. 3(a)

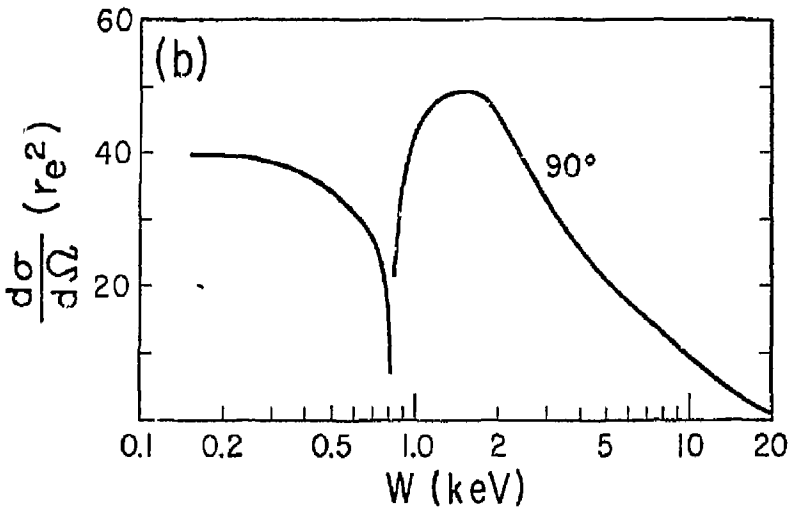

Fig.3(b)

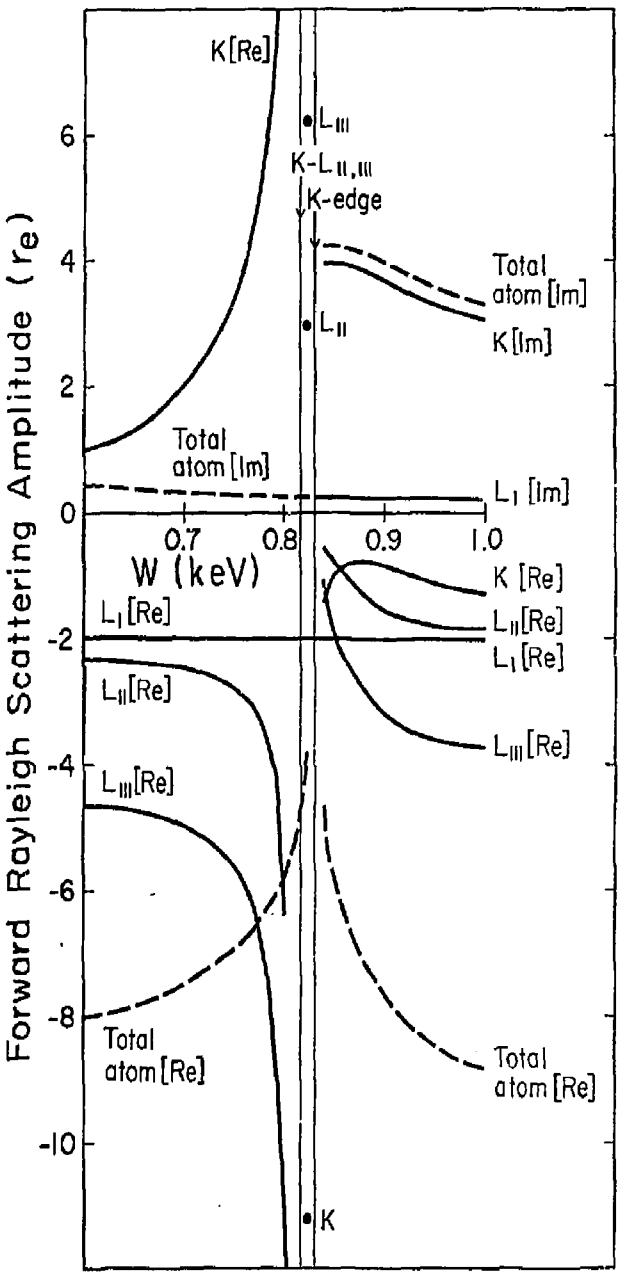
K[Re]
L_III
K-L_II,III
K-edge
Total atom [Im]
K[Im]
L_II
Total atom [Im]
L_I [Im]
Forward Rayleigh Scattering Amplitude (re)
6
4
2
0
-2
-4
-6
-8
-10
0.7
0.8
0.9
1.0
W (keV)
K [Re]
L_II[Re]
L_I[Re]
L_III[Re]
L_I[Re]
L_II[Re]
L_III[Re]
Total atom [Re]
Total atom [Re]
K

Fig. 4

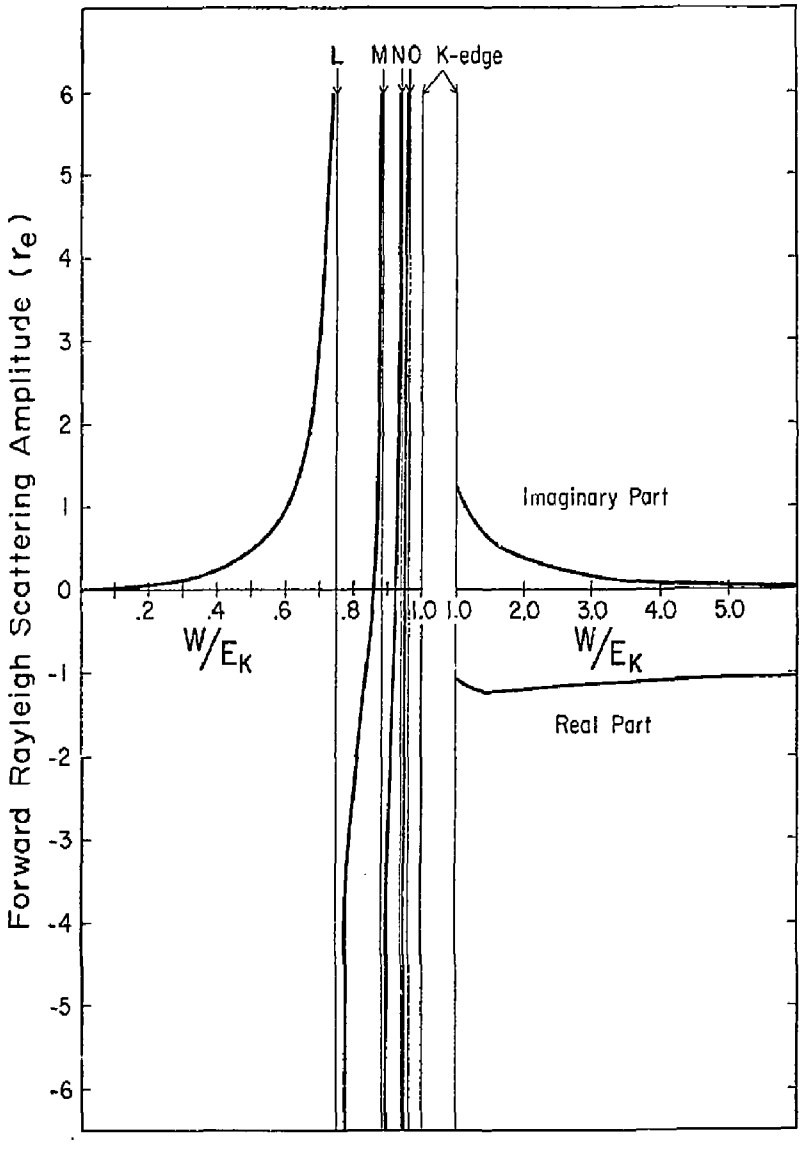
L
MNO
K-edge
Forward Rayleigh Scattering Amplitude (r_e)
6
5
4
3
2
1
0
-1
-2
-3
-4
-5
-6
.2
.4
.6
.8
1.0
1.0
2.0
3.0
4.0
5.0
W/E_K
W/E_K
Imaginary Part
Real Part

Fig.5

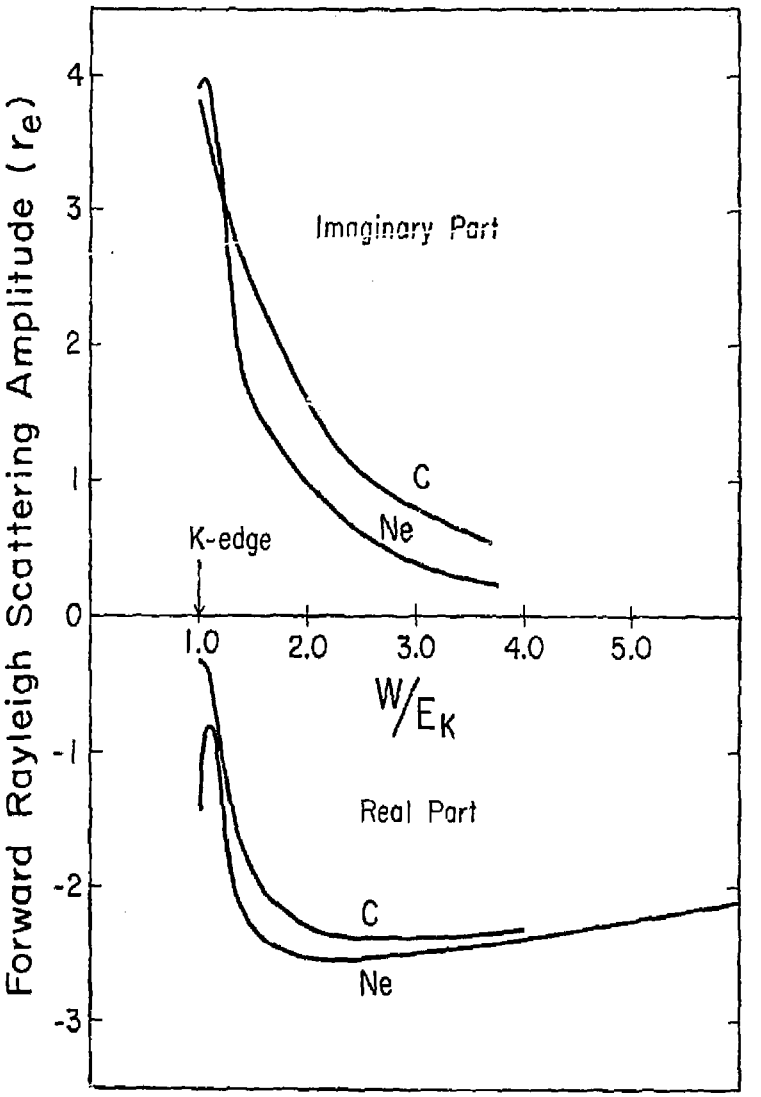
Forward Rayleigh Scattering Amplitude (r_e)
4
3
2
1
0
-1
-2
-3
Imaginary Part
C
Ne
K-edge
1.0
2.0
3.0
4.0
5.0
W/E_K
Real Part
C
Ne

Fig. 6

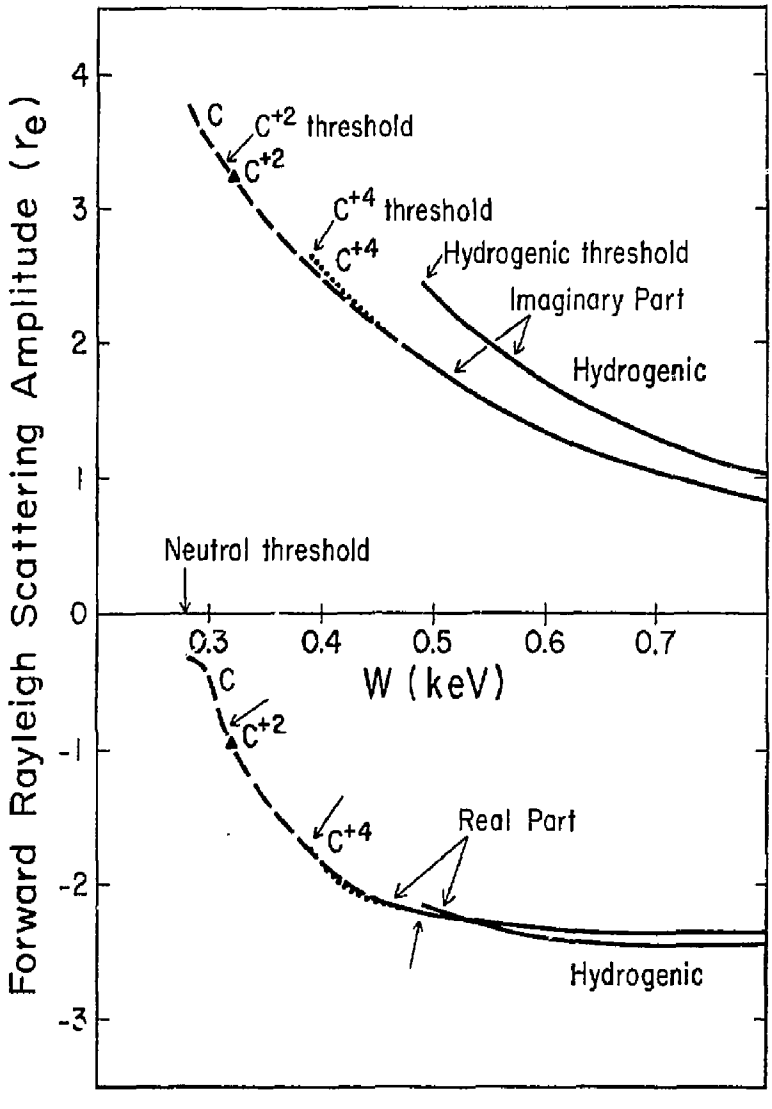
Forward Rayleigh Scattering Amplitude (r_e)
4
3
2
1
0
-1
-2
-3
C
C^{+2} threshold
C^{+2}
C^{+4} threshold
C^{+4}
Hydrogenic threshold
Imaginary Part
Hydrogenic
Neutral threshold
0.3
0.4
0.5
0.6
0.7
W (keV)
C
C^{+2}
C^{+4}
Real Part
Hydrogenic

Fig. 7